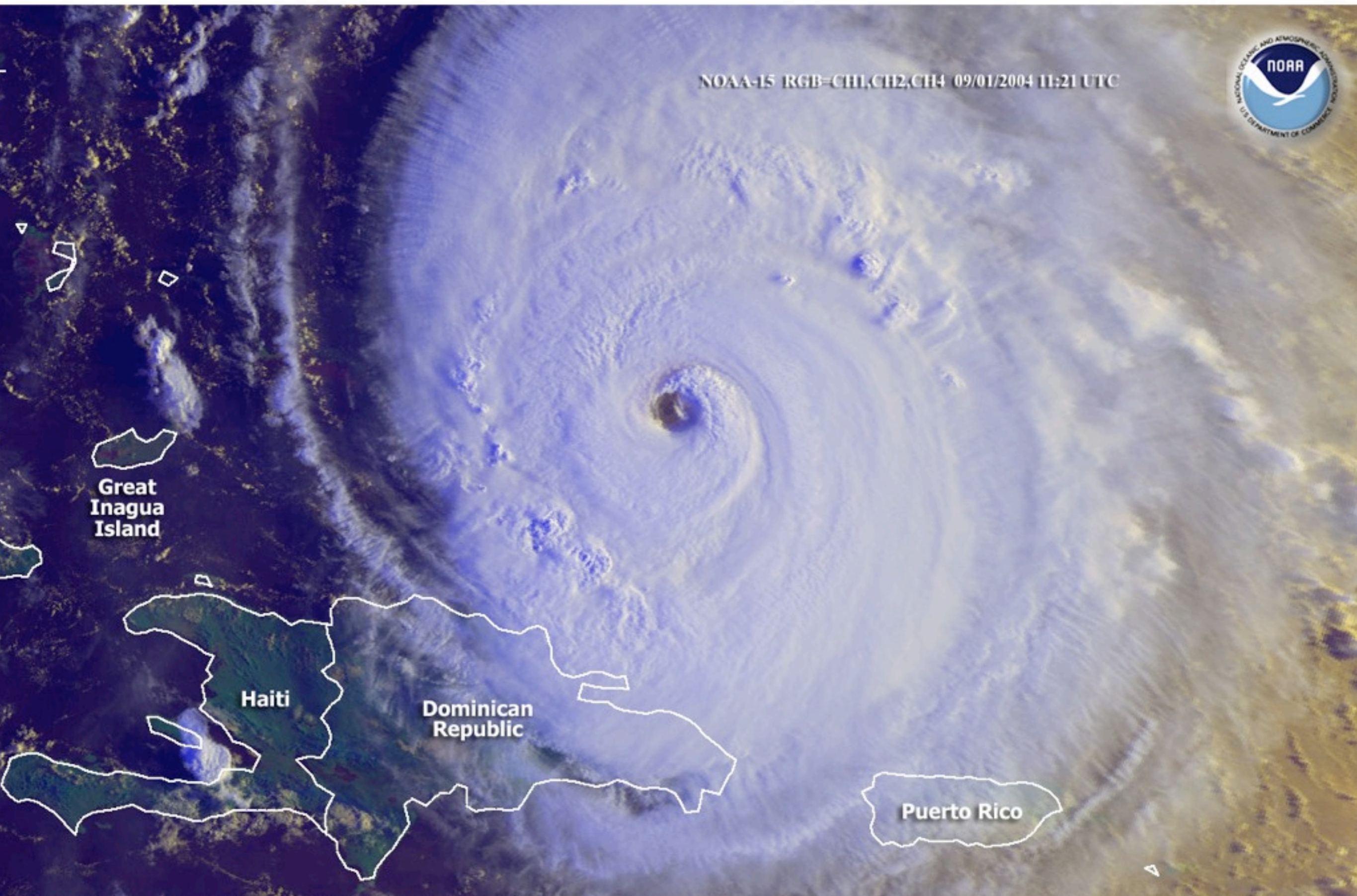


Category 4 Hurricane Frances is bearing down on the eastern Bahamas with maximum sustained winds near 140 mph and gusts to 165 mph.

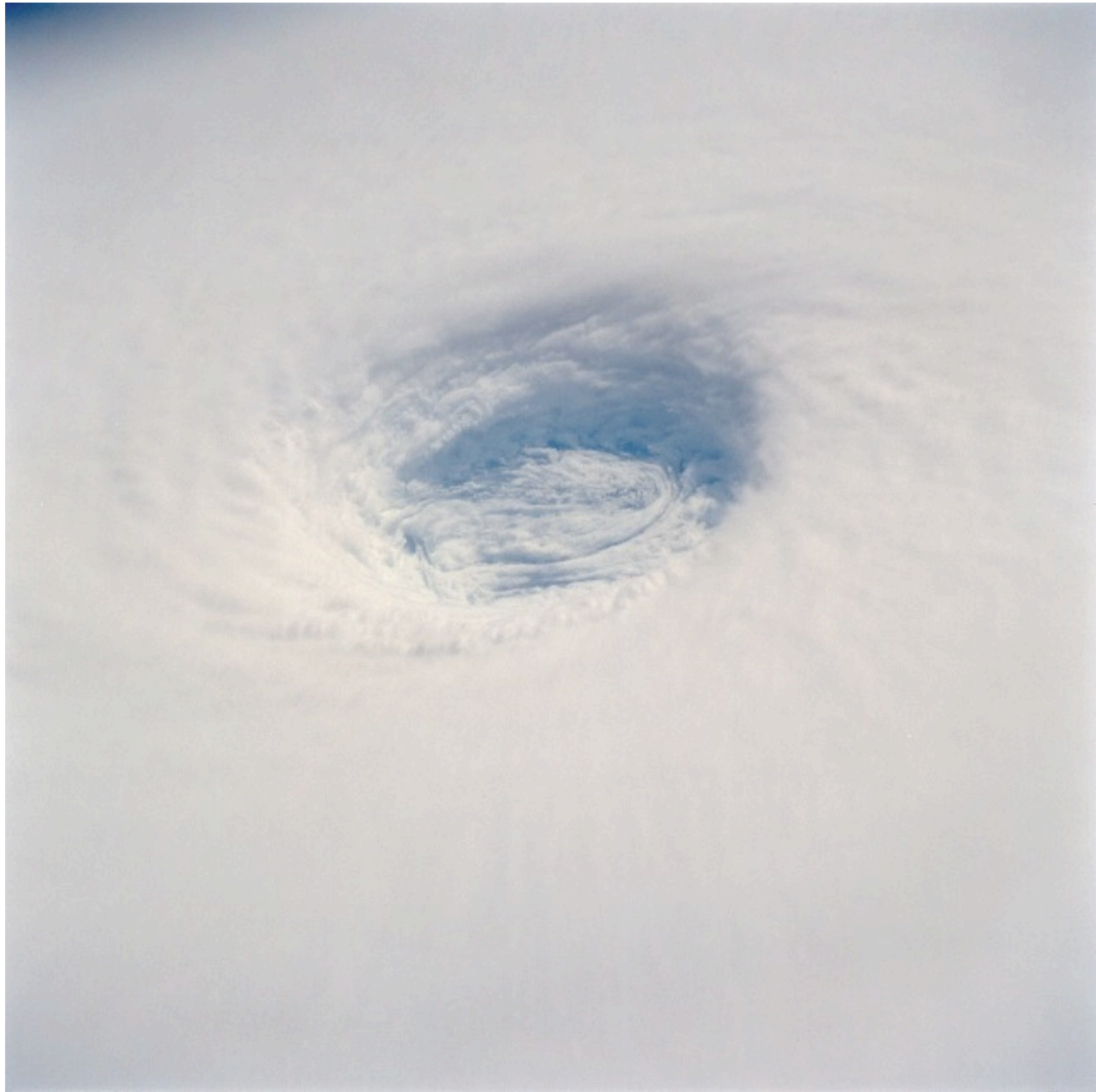
CREDIT: NOAA



NOAA-15 RGB=CH1,CH2,CH4 09/01/2004 11:21 UTC







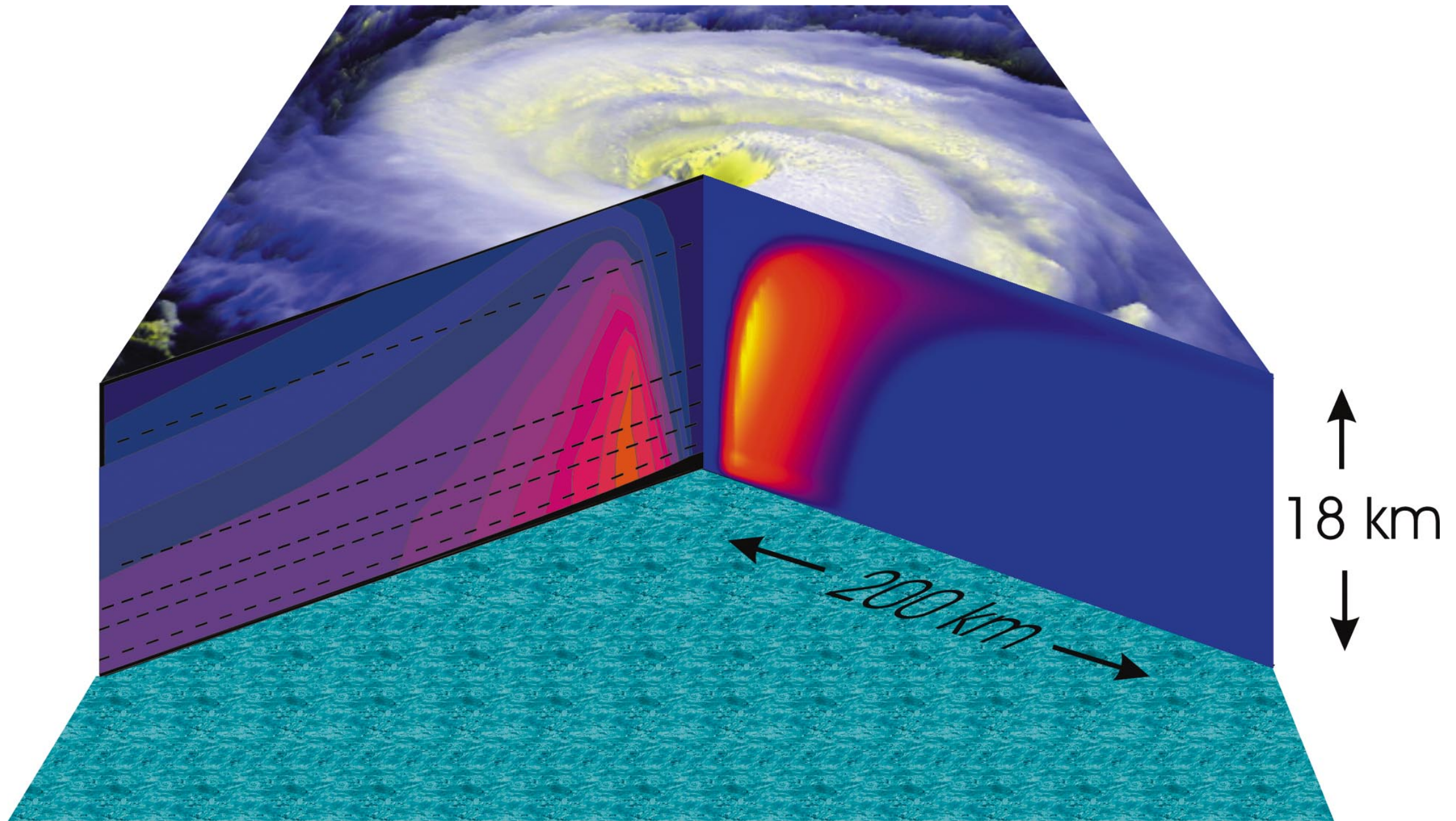


**Figure 3** Cutaway view of the structure of a tropical cyclone. The top of the storm is based on a satellite photograph of the cloud structure of Hurricane Fran of 1996. The right-hand cut shows the vertical component of velocity, from a numerical simulation of a hurricane using the model of Emanuel (1995a); maximum values (yellow) are approximately  $8 \text{ ms}^{-1}$ . The left-hand cut shows the magnitude of the tangential wind component measured in Hurricane Inez of 1966 by aircraft flying at levels indicated by the black dashed lines; from Hawkins & Imbembo (1976). Maximum values are approximately  $50 \text{ ms}^{-1}$ .

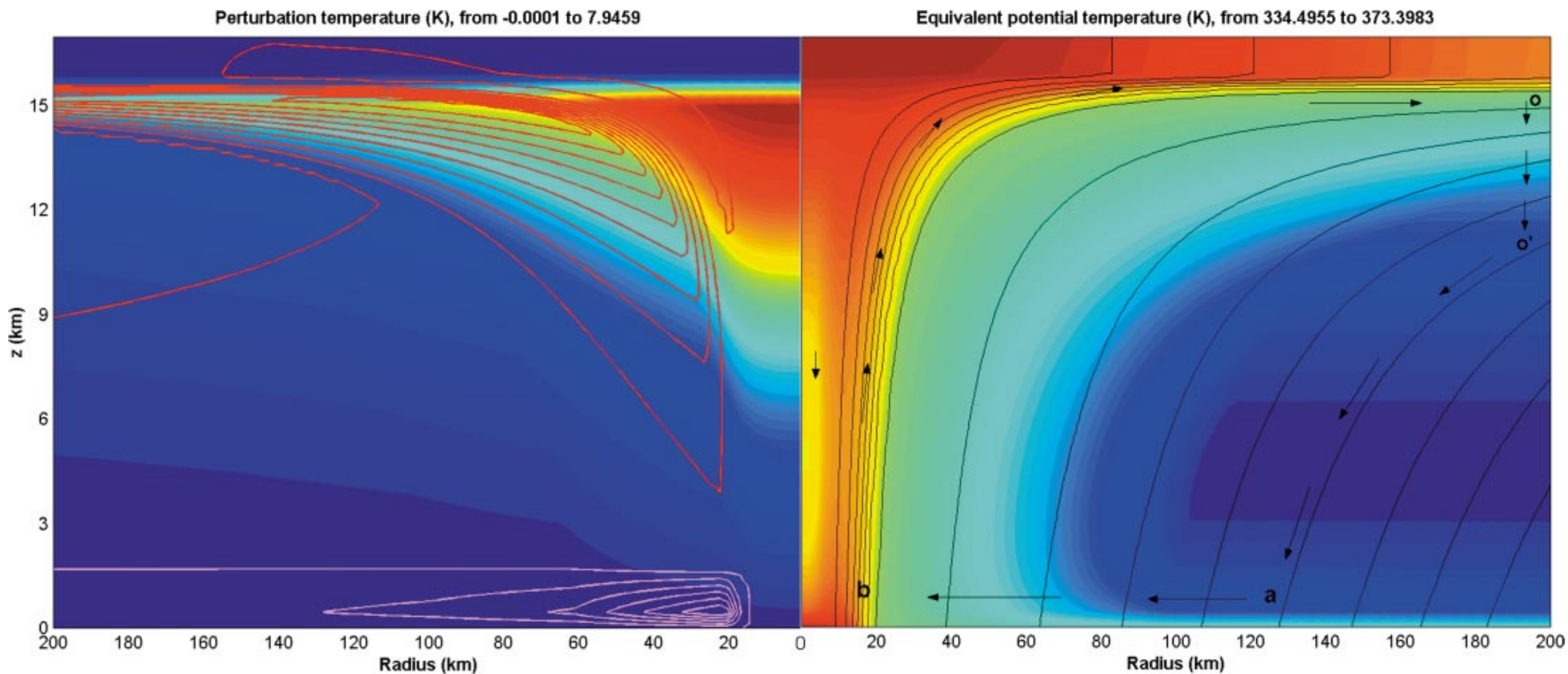


**Figure 4** Cross-section of a variety of quantities from a simple numerical model of a tropical cyclone (Emanuel 1995a). The right-hand panel shows a measure of the total specific entropy content of the air (shading), with blue colors denoting relatively small values and red colors showing larger values. The black contours show surfaces of constant absolute angular momentum per unit mass, about the axis of the storm, with values increasing outward. The arrows give an indication of the air motion in this plane. In the left-hand panel, the shading shows the temperature perturbation from the distant environment at the same altitude, with blue colors showing values near zero and red showing high values. The lavender contours near the bottom show the inward radial velocity, whereas the red contours closer to the top show outward radial velocity.

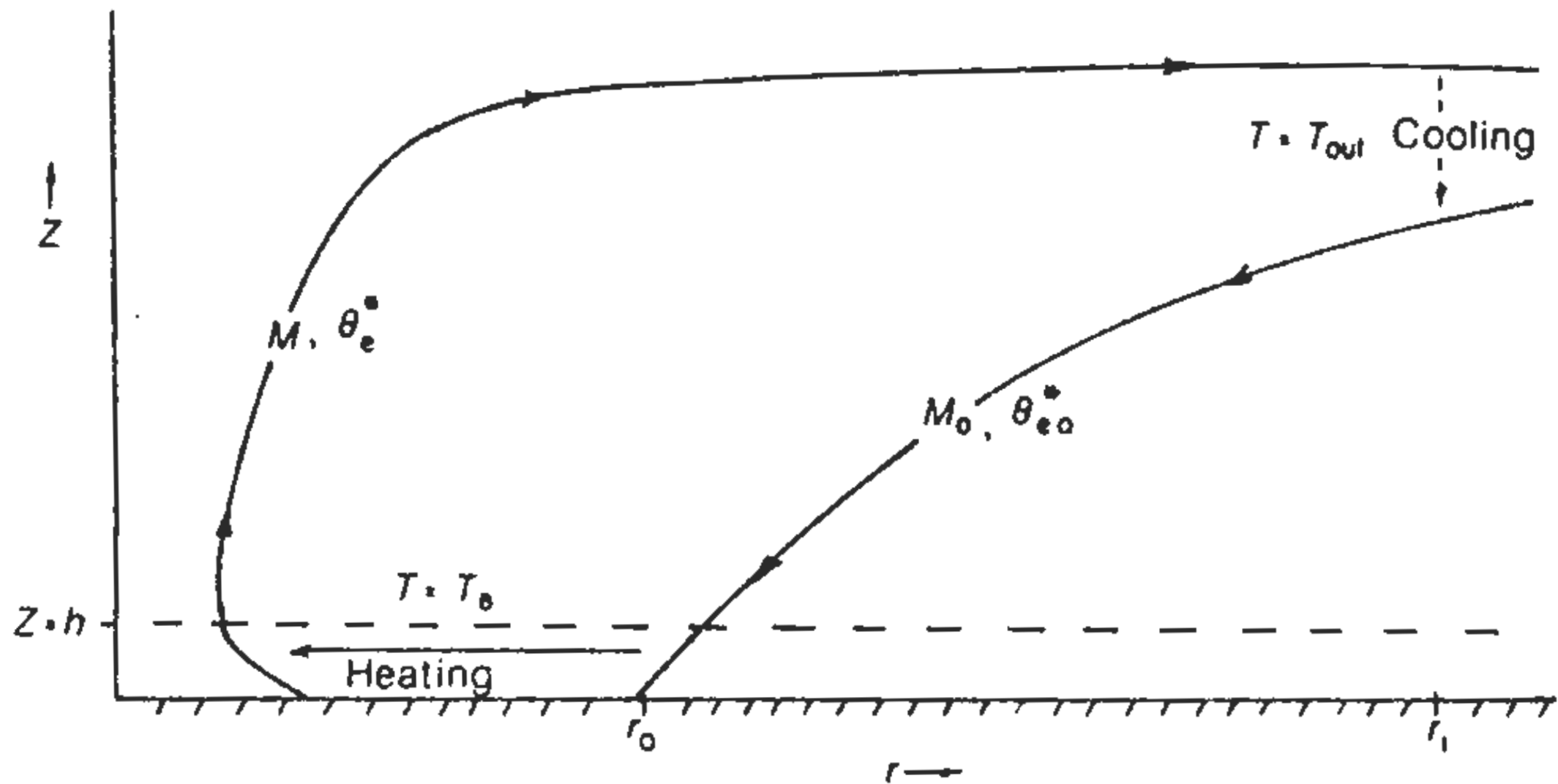


**Fig. 1** Carnot cycle of the mature tropical cyclone<sup>3</sup>. Air begins with absolute angular momentum per unit mass  $M_0$  and moist entropy  $\theta_{e0}^*$  at a radius  $r_0$ , and flows inward at constant temperature  $T_B$  within a thin boundary layer, where it loses angular momentum and gains moist entropy from the sea surface. It then ascends and flows outward to large radii, preserving its angular momentum ( $M$ ) and moist entropy ( $\theta_e^*$ ). Eventually, at large radii, the air loses moist entropy by radiative cooling to space at a mean temperature  $T_{out}$  and acquires angular momentum by interaction with the environment.

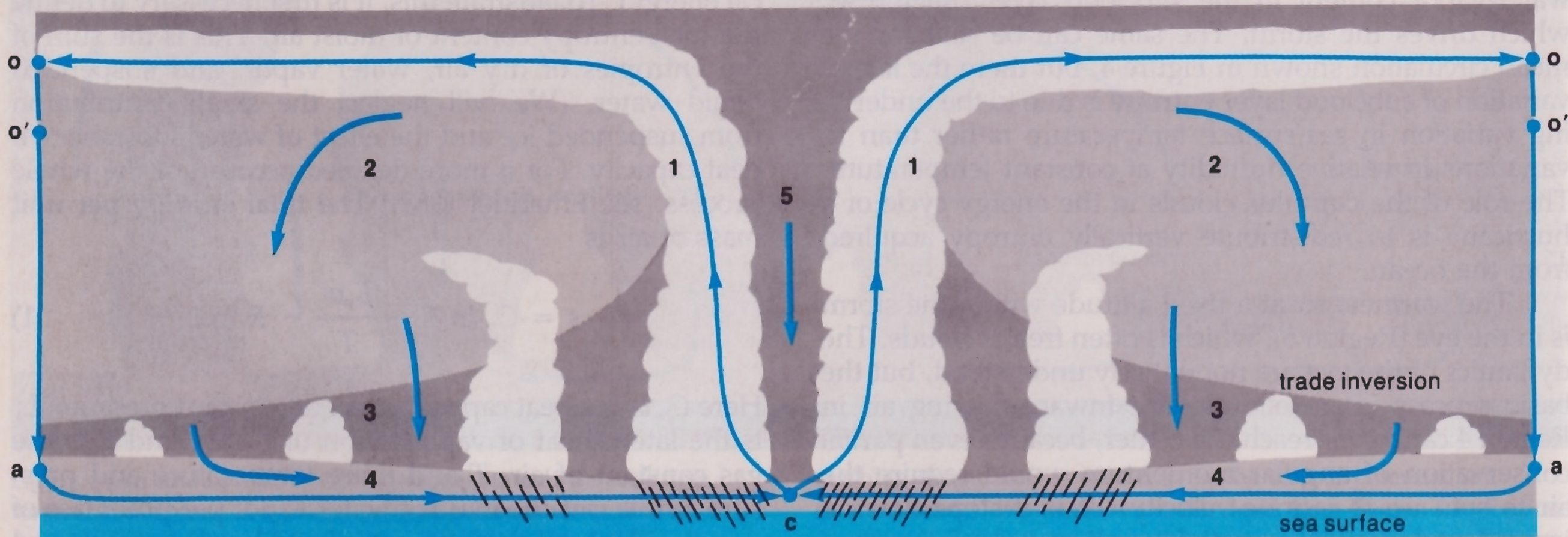
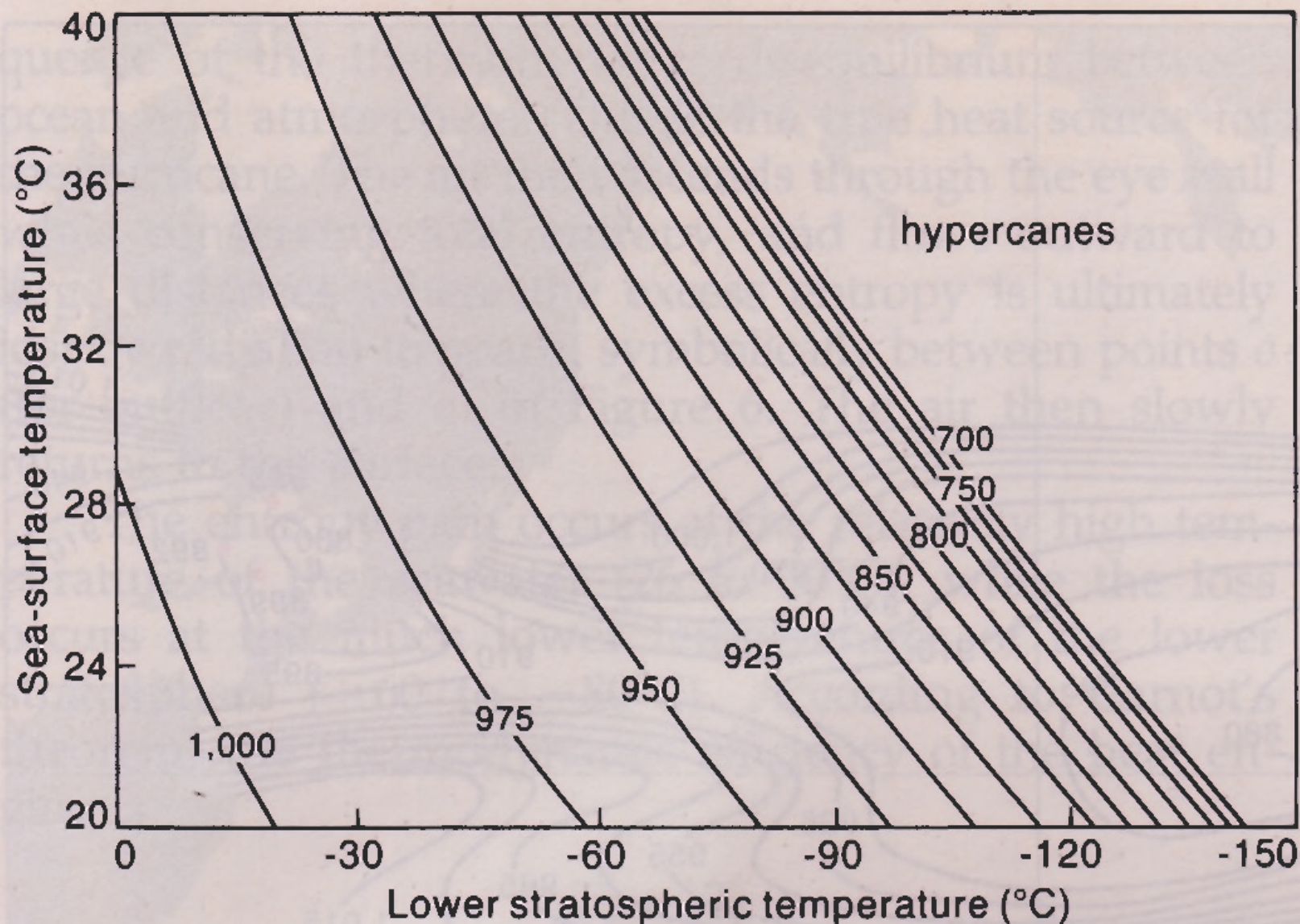


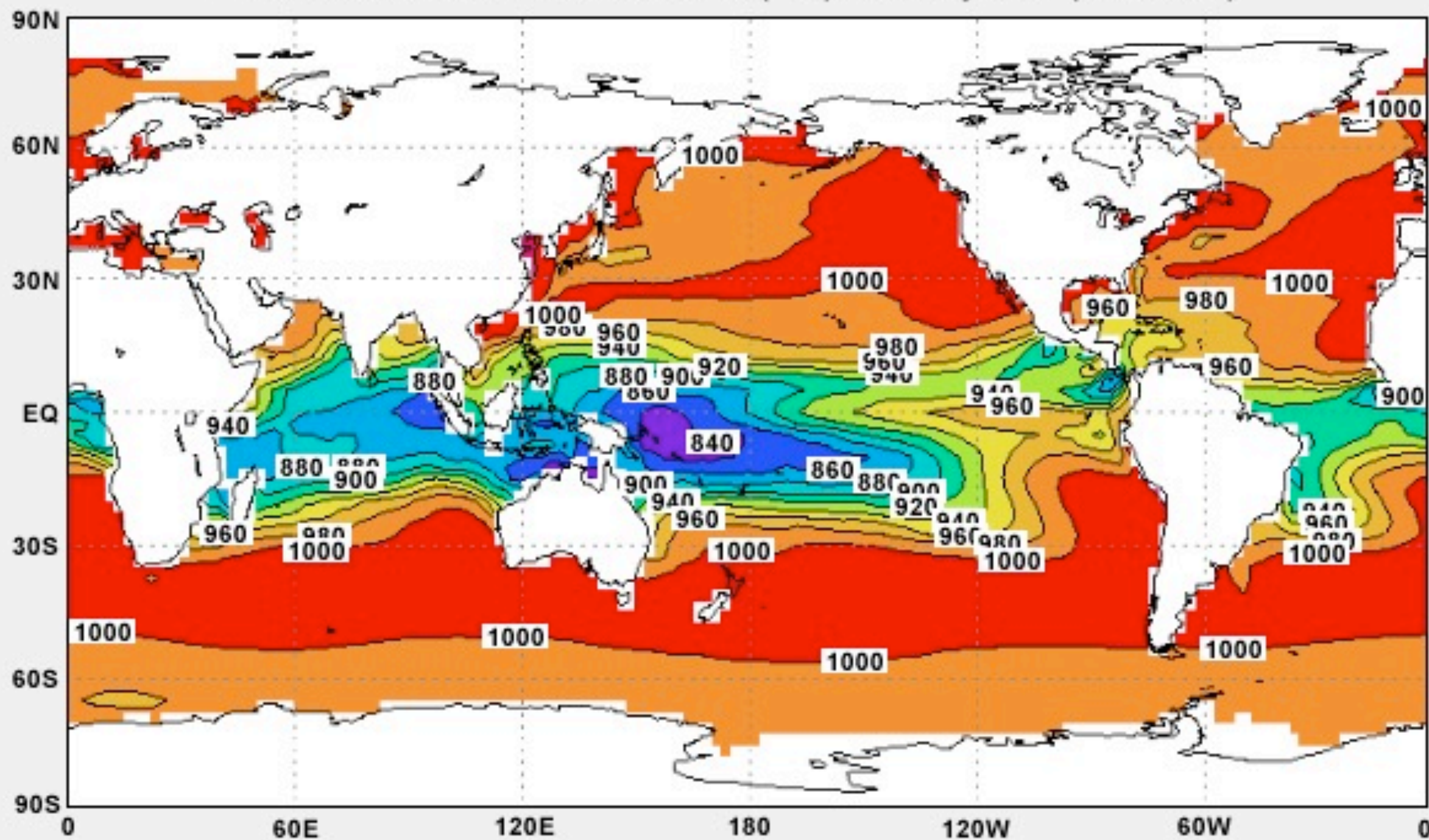
Figure 6. The structure and airflow of a mature hurricane are shown in this cross section, which spans a width of about 1,600 km and a height of 15 km. The regions correspond closely to those of the overall tropical atmosphere shown in Figure 4, but with an additional region of subsiding air in the eye (Region 5). In this case, the sea-surface temperature may be considered constant, but the total entropy content of the subcloud layer (Region 4) increases inward toward the eye as the increasing surface wind speed leads to greater evaporation rates, causing the near-surface air to approach

saturation. The total entropy increases from point *a* to point *c* and is approximately conserved during ascent through the eye wall to point *o*. Heat is lost by infrared radiation to space, symbolically between points *o* and *o'*. Because heat is acquired at a much higher temperature than it is lost at, the Carnot heat engine, which converts heat into mechanical energy, is very efficient ( $\epsilon \approx 1/3$ ). In the steady state, this energy is mostly balanced by frictional dissipation at the surface.



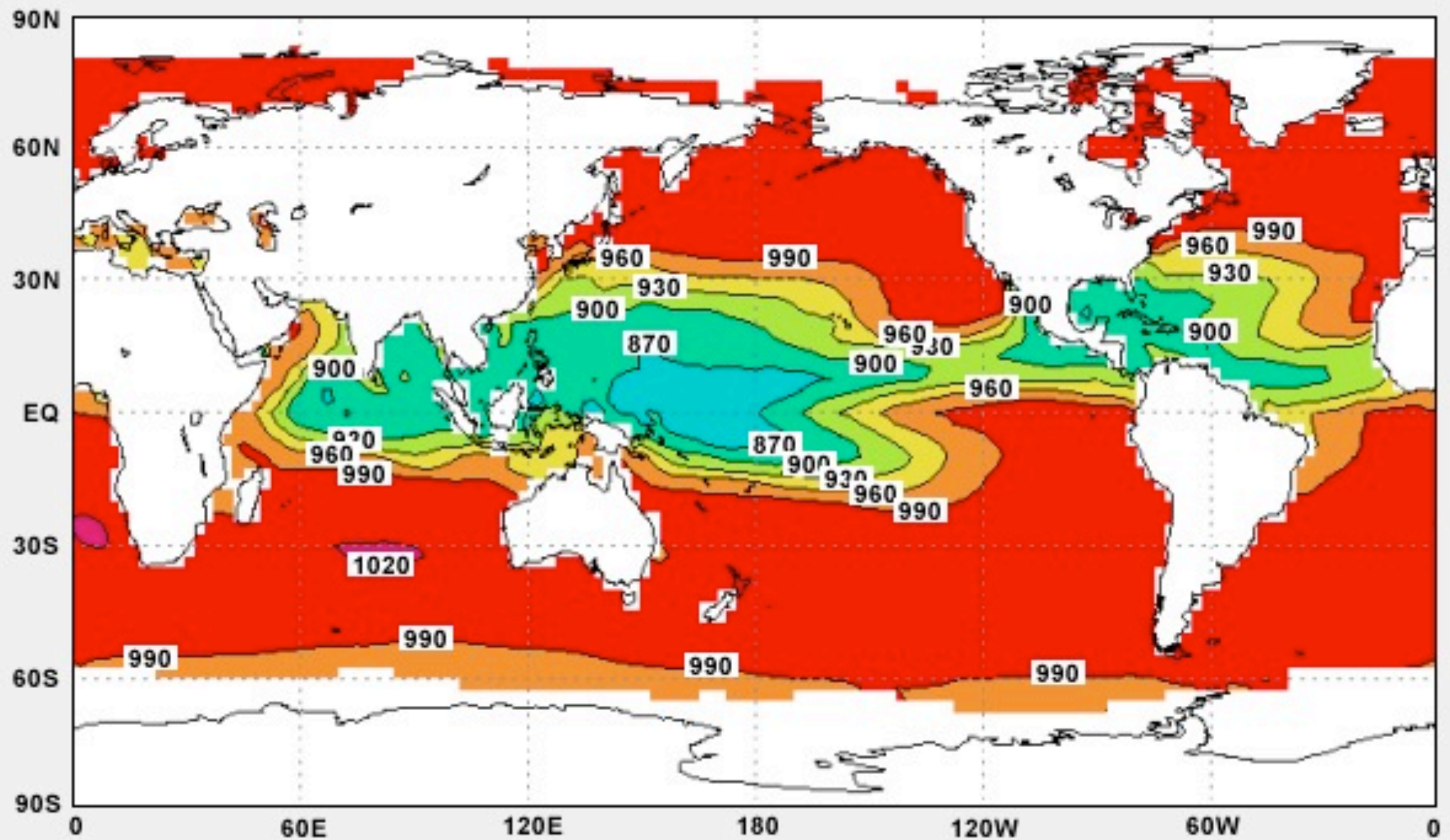
**Figure 8.** A more general way to assess the low atmospheric pressures associated with hurricanes is demonstrated by this diagram, which shows the minimum sustainable central pressure (in millibars) of tropical storms calculated from Eq. 5 as a function of the sea-surface temperature and the mean temperature of the lower stratosphere. The ambient surface relative humidity is assumed to be 75%. No solutions of Eq. 5 are possible in the region marked "hypercanes" because the mechanical energy produced by the Carnot heat engine is so large that it cannot be balanced by surface friction alone. The intensity of hurricanes in this regime would be limited by internal turbulent dissipation of kinetic energy, presumably at very high wind speeds.

Minimum Sustainable Surface Pressure (hPa): February Mean (1982-1995)



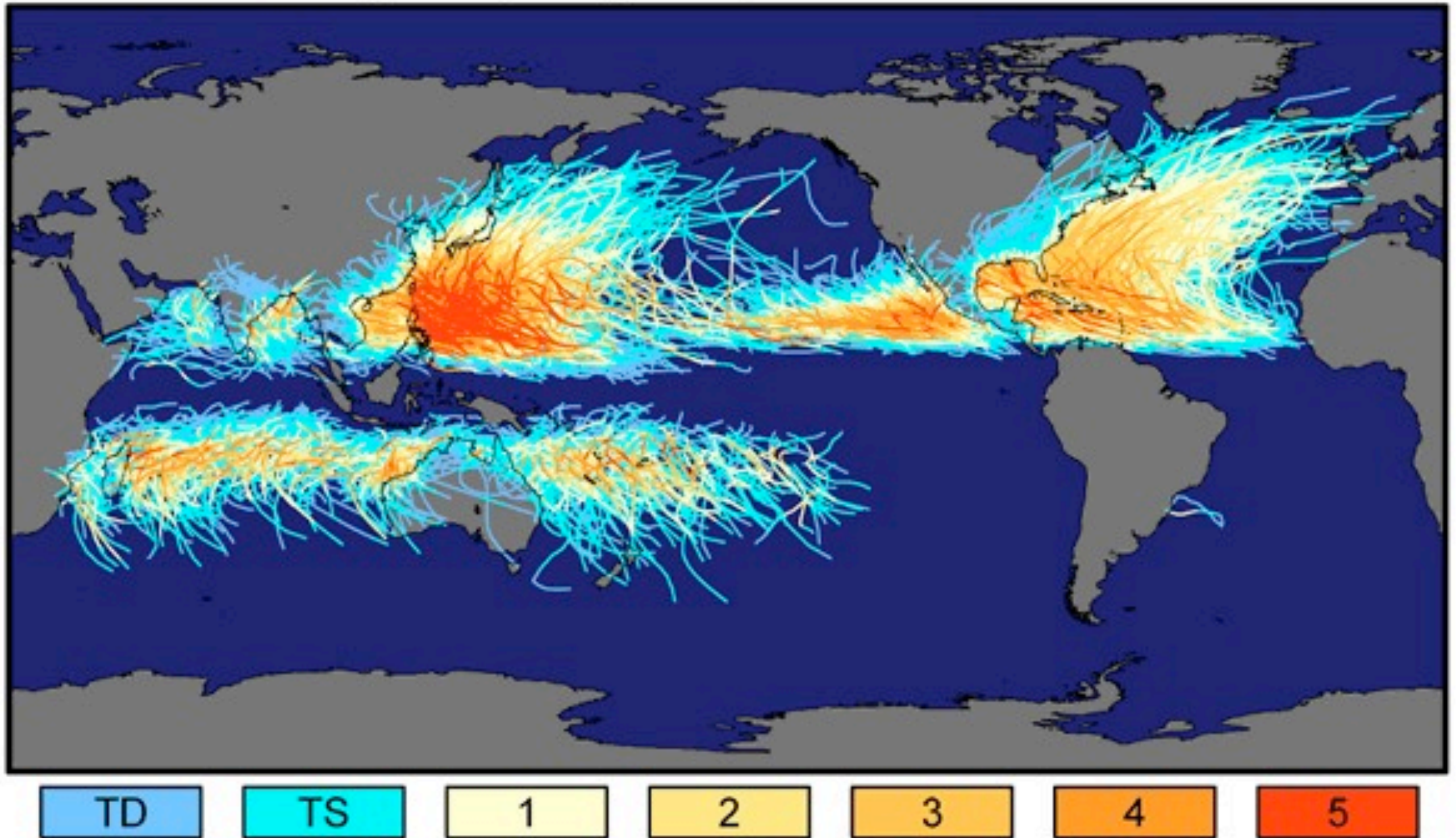
Kerry Emanuel, MIT

Minimum Sustainable Surface Pressure (hPa): September Mean (1982-1995)



Kerry Emanuel, MIT

# Tracks and Intensity of Tropical Cyclones, 1851-2006



Saffir-Simpson Hurricane Intensity Scale

**An Air-Sea Interaction Theory for Tropical Cyclones. Part II: Evolutionary Study Using a Nonhydrostatic Axisymmetric Numerical Model**

**RICHARD ROTUNNO**

*National Center for Atmospheric Research\*, Boulder, CO 80307*

**KERRY A. EMANUEL**

*Center for Meteorology and Physical Oceanography, Massachusetts Institute of Technology, Cambridge, MA 02139*

*(Manuscript received 17 April 1986, in final form 17 September 1986)*

## 2. Description of the model

The governing equations for compressible, axisymmetric flow on an  $f$ -plane in the cylindrical coordinates  $(r, \phi, z)$  are

*Momentum:*

$$\frac{du}{dt} - \left(f + \frac{v}{r}\right)v = -c_p \bar{\theta}_v \frac{\partial \pi}{\partial r} + D_u \quad (1)$$

$$\frac{dv}{dt} + \left(f + \frac{v}{r}\right)u = D_v \quad (2)$$

$$\frac{dw}{dt} = -c_p \bar{\theta}_v \frac{\partial \pi}{\partial z} + D_w$$

$$+ g \left\{ \frac{\theta - \bar{\theta}}{\bar{\theta}} + 0.61(q_v - \bar{q}_v) - q_l \right\} \quad (3)$$

*Conservation of mass:*

$$\frac{\partial \pi}{\partial t} + \frac{\bar{c}^2}{c_p \bar{\rho} \bar{\theta}_v^2} \left\{ \frac{1}{r} \frac{\partial (ru \bar{\rho} \bar{\theta}_v)}{\partial r} + \frac{\partial (w \bar{\rho} \bar{\theta}_v)}{\partial z} \right\} = 0 \quad (4)$$

*First Law of Thermodynamics:*

$$\frac{d\theta}{dt} = M_\theta + D_\theta + R \quad (5)$$

*Conservation of water vapor:*

$$\frac{dq_v}{dt} = M_{q_v} + D_{q_v} \quad (6)$$

*Conservation of liquid water:*

$$\frac{dq_l}{dt} = M_{q_l} + D_{q_l} \quad (7)$$

## *a. Microphysics*

The effects of phase changes of water substance are represented by

$$M_{\theta} = -\frac{L}{c_p \pi} \frac{dq_{vs}}{dt} \quad (8)$$

$$M_{q_v} = \frac{dq_{vs}}{dt} \quad (9)$$

$$M_{q_l} = -\frac{dq_{vs}}{dt} + \frac{1}{\bar{\rho}} \frac{\partial(\bar{\rho} V q_l)}{\partial z}, \quad (10)$$

The only distinction between cloud water and rain water is the terminal velocity,  $V$ . For  $q_l \leq 1$  g/kg,  $V = 0$ , while for  $q_l > 1$  g/kg,  $V = 7$  m/s.

# Turbulence

- As in a slab-symmetric 2D model, the assumption of axisymmetry allows no direct calculation of turbulent motions, to the extent that real turbulence is 3D.
- In an axisymmetric (or 2D) model, *all* turbulent motion is parameterized, so that higher resolution in a model so constrained does not tell anything more about turbulent motions, it only gives more detail about the simulated flow that is axisymmetric.
- The representation of turbulence is essentially the same as described in the turbulence closure model presented on Day 17, but in cylindrical coordinates.

# Radiation

“Radiative cooling” is crudely represented by Newtonian cooling,

$$R = -\frac{\theta - \bar{\theta}}{\tau_R},$$

which relaxes the temperature toward the initial state rather than toward a state of radiative equilibrium. This is an expedient which allows the environment to remain similar to the mean hurricane environment.

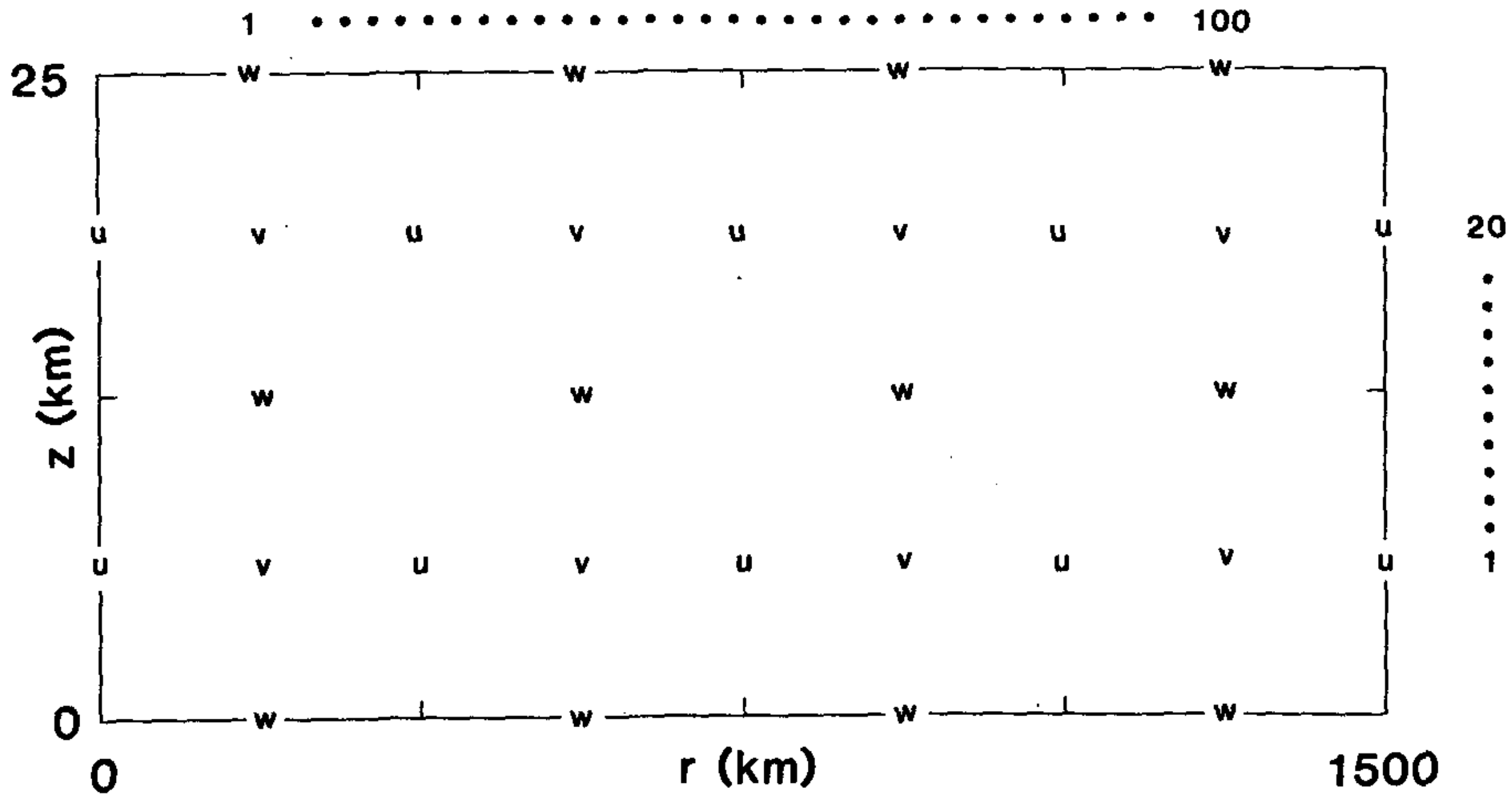


FIG. 1. Domain and arrangement of dependent variables on the staggered grid covering the domain. All "thermodynamic" variables are located at the  $v$  points.

# Boundary Conditions

- To damp gravity waves before they can reflect from the upper boundary (a rigid lid), use a ``sponge'' layer in the upper part of the domain.
- To allow gravity waves produced by cumulus convection in the outer regions of the vortex to propagate radially out of the domain, use a radiation b.c. like that used for mountain wave simulations.

At the lower surface we require that the normal velocity vanish ( $w = 0$ ). The tangential stresses and vertical fluxes at the surface are given by the bulk aerodynamic formulas:

$$\tau_{rz} = [C_D u (u^2 + v^2)^{1/2}]_{\Delta z/2} \quad (32)$$

$$\tau_{z\phi} = [C_D v (u^2 + v^2)^{1/2}]_{\Delta z/2} \quad (33)$$

$$F_z^\theta = [C_E (u^2 + v^2)^{1/2}]_{\Delta z/2} (\theta_{\text{surf}} - \theta|_{\Delta z/2}) \quad (34)$$

$$F_z^{q_v} = \{C_E \sqrt{u^2 + v^2}\}_{\Delta z/2} (q_{v \text{ surf}} - q_v|_{\Delta z/2}). \quad (35)$$

$C_D$  and  $C_E$  are the drag coefficients for momentum and heat (sensible and latent), respectively, which, unless otherwise mentioned, are taken to be equal and given by Deacon's formula,

$$C_D = 1.1 \times 10^{-3} + 4 \times 10^{-5} (u^2 + v^2)^{1/2}|_{\Delta z/2} \quad (36)$$

# Initial Conditions

- Neutral to the model's convection
- Specify the vortex tangential velocity:

$$v(r, z, 0) = \frac{z_{\text{sponge}} - z}{z_{\text{sponge}}} \left( \left\{ v_m^2 \left( \frac{r}{r_m} \right)^2 \left[ \left( \frac{2r_m}{r + r_m} \right)^3 - \left( \frac{2r_m}{r_0 + r_m} \right)^3 \right] + \frac{f^2 r^2}{4} \right\}^{1/2} - \frac{fr}{2} \right) \quad (37)$$

- Adjust temperature field so that it is in thermal wind balance.

TABLE 2. Numerical experiments.

Exp	Initial vortex			$T_{\text{surf}}$ (°C)	Tropopause (mb)	Comments
	$u_{\text{max}}$ (m s <sup>-1</sup> )	$r_m$ (km)	$r_0$ (km)			
A	12	82.5	412.5	26.3	100	Control run
B	2	82.5	412.5	26.3	100	Weak vortex
C	12	160.0	800.0	26.3	100	Large vortex
D	12	41.0	206.0	26.3	100	Small vortex $\Delta r = 7.5$ km, $r_{\text{outer}} = 750$ km, $l_H = 1500$ m
E	12	82.5	412.5	26.3	100	Dry to 30% RH above boundary layer
F	12	82.5	412.5	26.3	300	Increase tropopause
G	12	82.5	412.5	31.3	100	Increase SST
H	12	82.5	412.5	31.3	200	Increase SST and lower tropopause
I	12	82.5	412.5	31.3	300	Increase SST and lower tropopause
J	12	82.5	412.5	26.3	100	Limited Newtonian cooling $ R  < 2$ K d <sup>-1</sup>
K	12	82.5	412.5	26.3	100	Zero Newtonian cooling $R = 0$

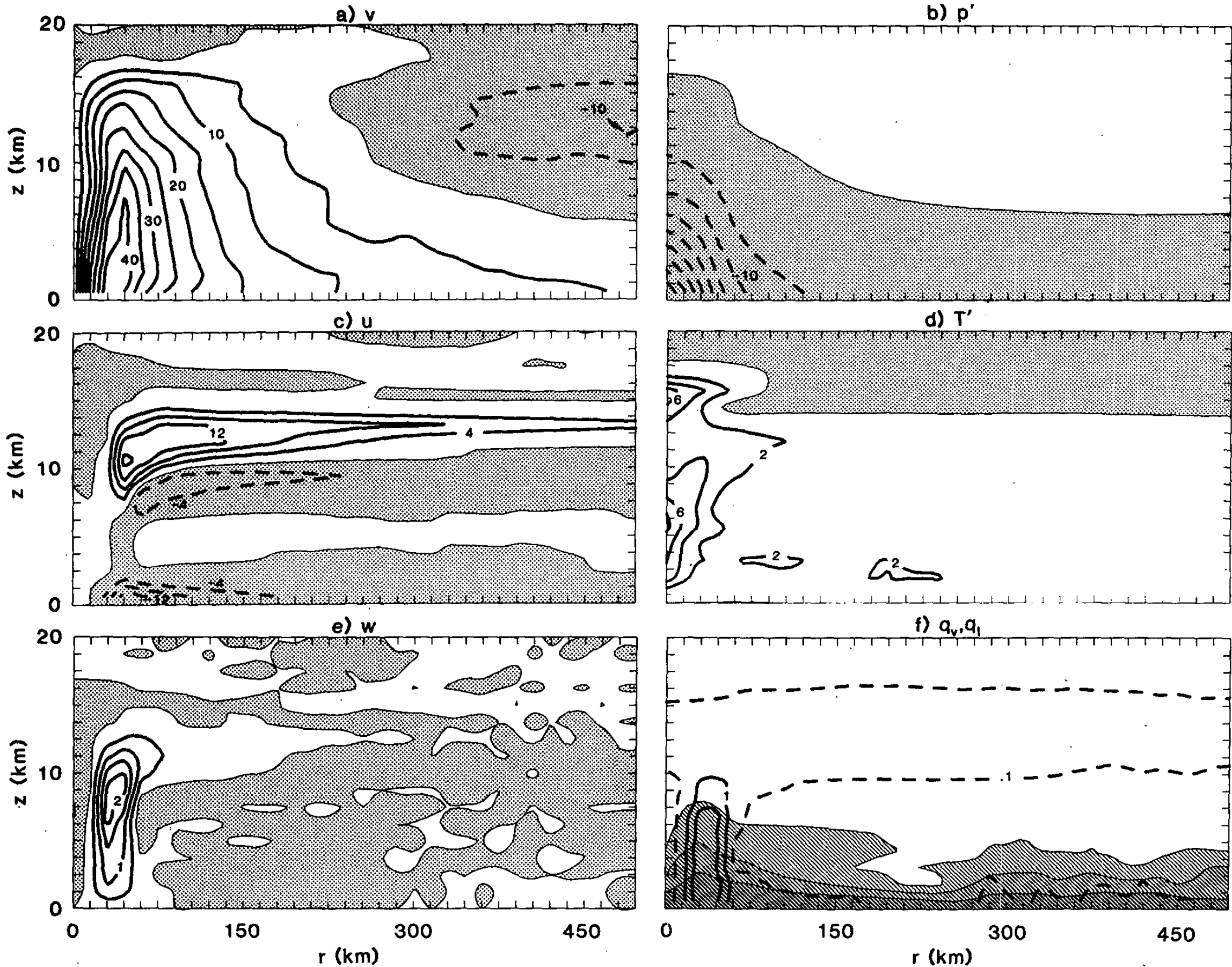


FIG. 5. The 160–180 h average fields for the nearly steady state reached in the control run. All stippled regions indicate negative values of the field (a) Azimuthal velocity, contour interval,  $5 \text{ m s}^{-1}$ ; (b) dimensional pressure deviation from the initial state, contour interval,  $5 \text{ mb}$ ; (c) radial velocity, contour interval,  $4 \text{ m s}^{-1}$ ; (d) temperature deviation from the initial state, contour interval,  $2 \text{ K}$ ; (e) vertical velocity, contour interval,  $0.5 \text{ m s}^{-1}$ ; (f) liquid water, contour interval,  $1 \text{ g kg}^{-1}$ ; dashed line denotes the  $0.1 \text{ g kg}^{-1}$  contour, and water vapor; lightest shading indicates  $3 < q_v < 8 \text{ g kg}^{-1}$ , dashed shading indicates  $8 < q_v < 13 \text{ g kg}^{-1}$ , and darkest shading indicates  $q_v > 13 \text{ g kg}^{-1}$ .

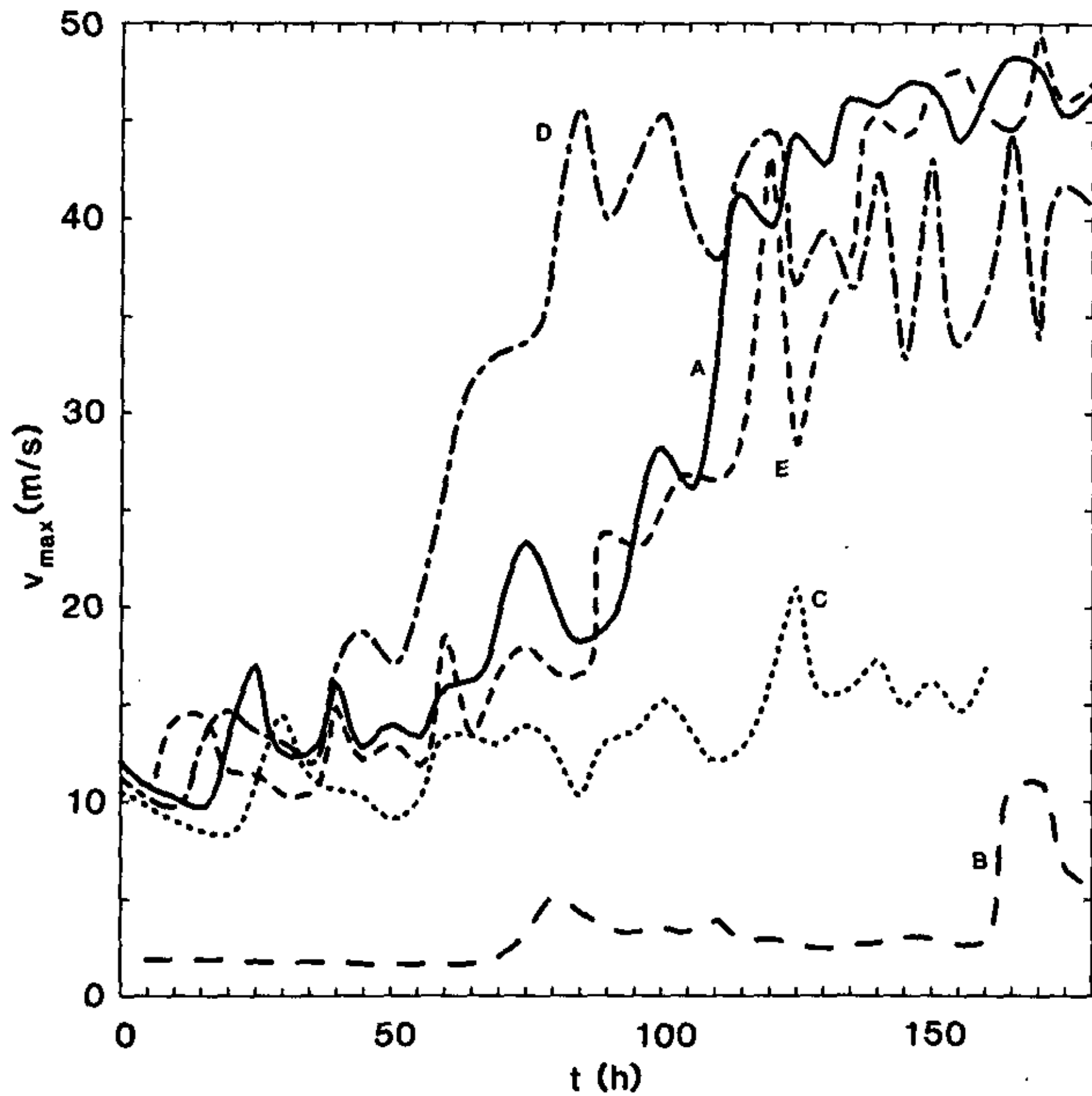
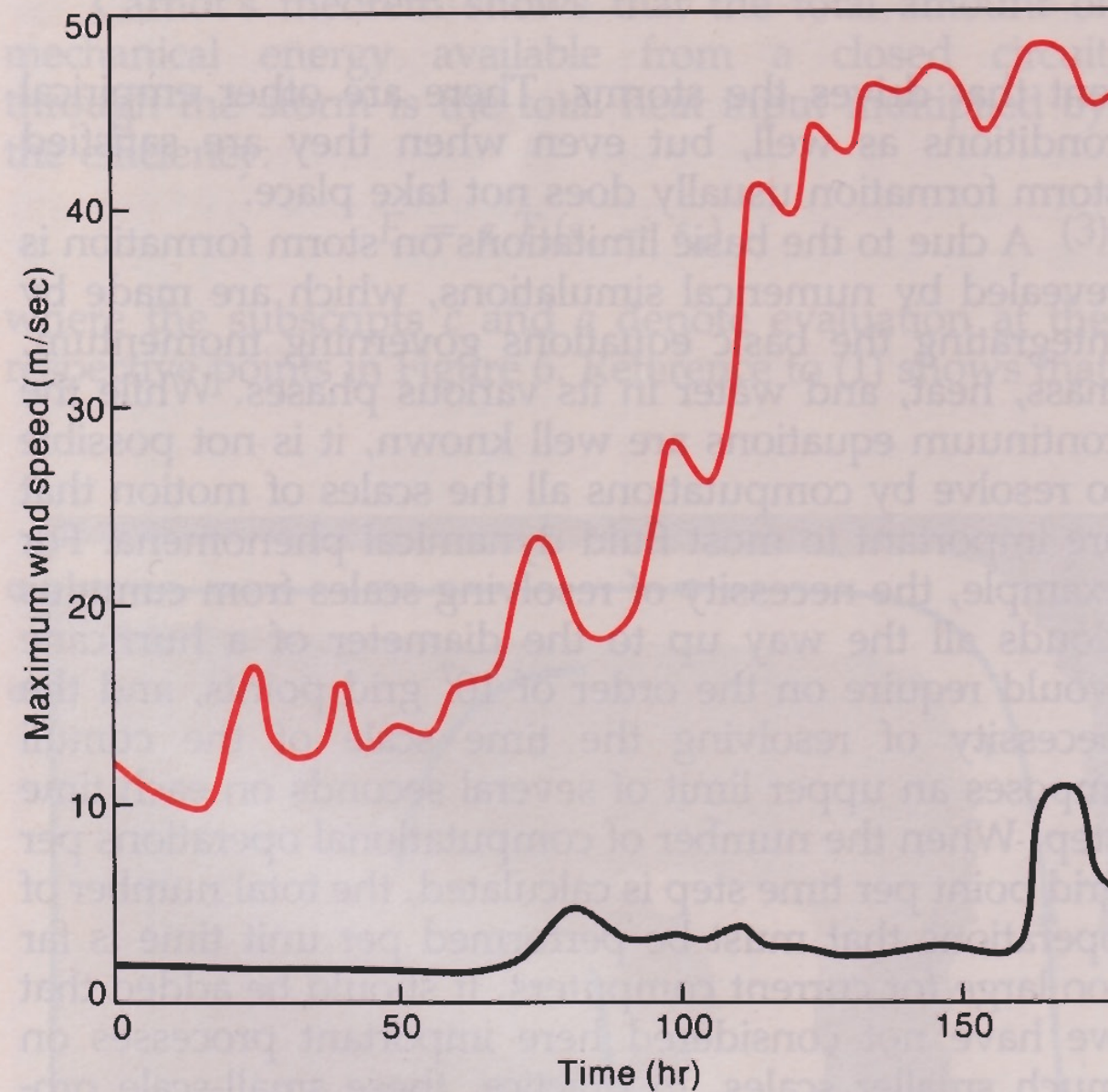


FIG. 3. Time series of  $v_{\max}$  for Exps. A-E (defined in Table 2).



**Figure 9. Computer models provide a partial answer to the question of why hurricanes are rare even though the tropical atmosphere has abundant energy to support them. This graph shows the evolution with time of the maximum surface wind speed produced by one such numerical model (Rotunno and Emanuel 1987). The red curve begins with a 12 m/sec amplitude vortex, while the maximum velocity in an experiment that starts with a 2 m/sec amplitude vortex, but is otherwise identical, is shown by the gray curve. The failure of the weak vortex to amplify demonstrates that hurricanes in this model cannot arise out of weak random noise; rather, a vortex of sufficient amplitude must be provided by independent means, such as a large-scale wave or a thunderstorm complex from a middle-latitude continent.**

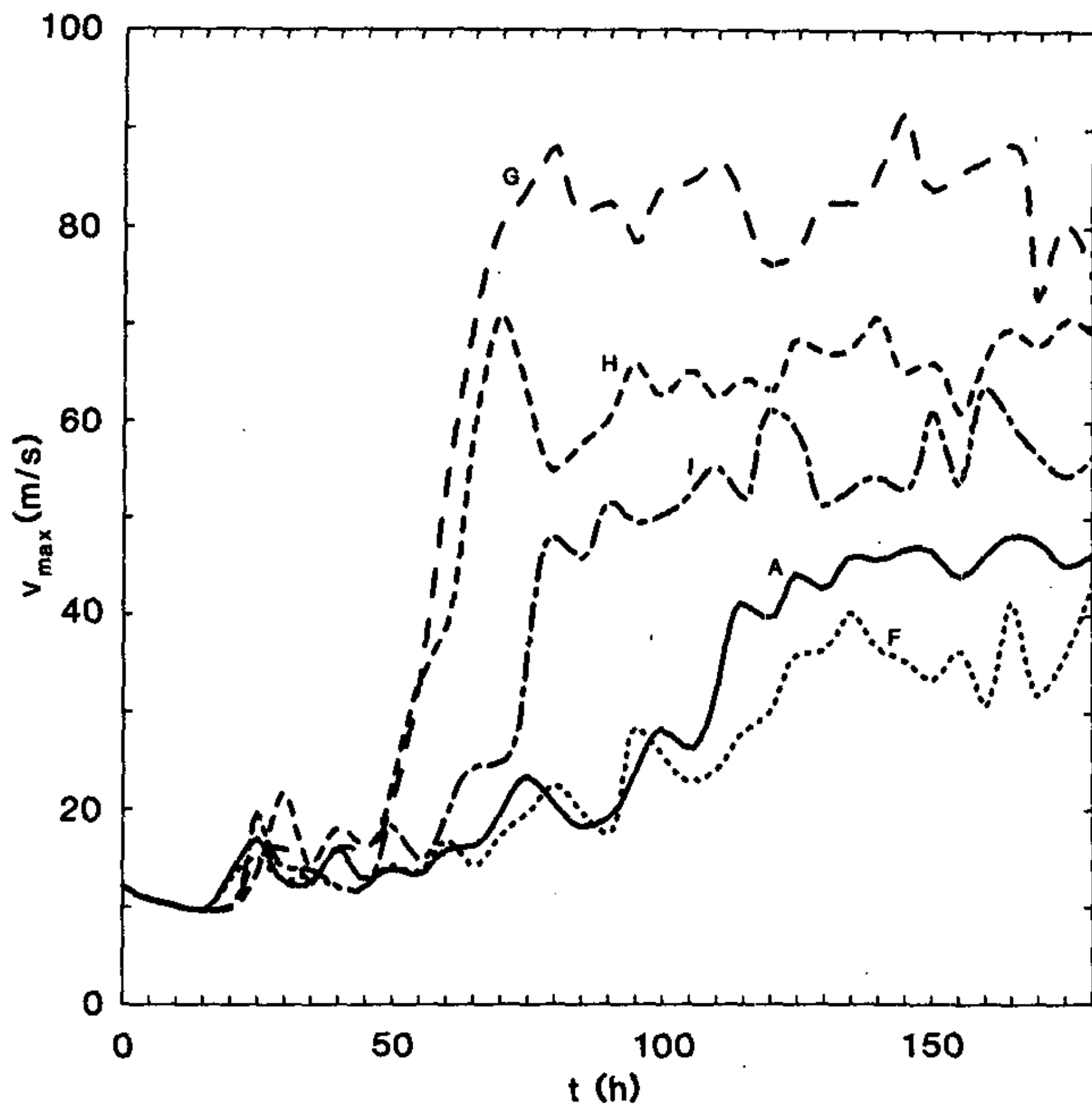


FIG. 7. Time series of  $v_{\max}$  for Exps. A, F, G, H and I (defined in Table 2).

TABLE 3. Comparison of theory and numerical experiment.

Exp	Numerical experiments*										Theory		
	$T_8$ (°C)	$\bar{T}_{out}$ (K)	$(\bar{T}_{out})_{est}^\dagger$ (K)	$T_B$ (K)	$\epsilon$	$r_{max}$ (km)	$r_0$ (km)	$RH_{as}$ (%)	$p_c$ (mb)	$v_{max}$ (m s <sup>-1</sup> )	$p_c$ (mb)	$v_{max}$ (m s <sup>-1</sup> )	$r_0$ (km)
A	26.3	228	203	295.	.23	38	400	81.8	973	46	975	48	380
F	26.3	245	244	295.	.17	45	400	81.8	991	38	989	42	340
G	31.3	207	197	298.	.31	30	900	78.6	903	77	903	72	570
H	31.3	227	227	298.5	.24	40	750	78.6	937	66	944	63	490
I	31.3	246	246	298.5	.18	50	700	78.6	964	55	972	54	430
J	26.3	216	203	295.	.27	38	340	81.8	961	51	961	53	440
K	26.3	212	203	295.	.28	38	370	81.8	957	57	956	59	450

# The Carnot Cycle

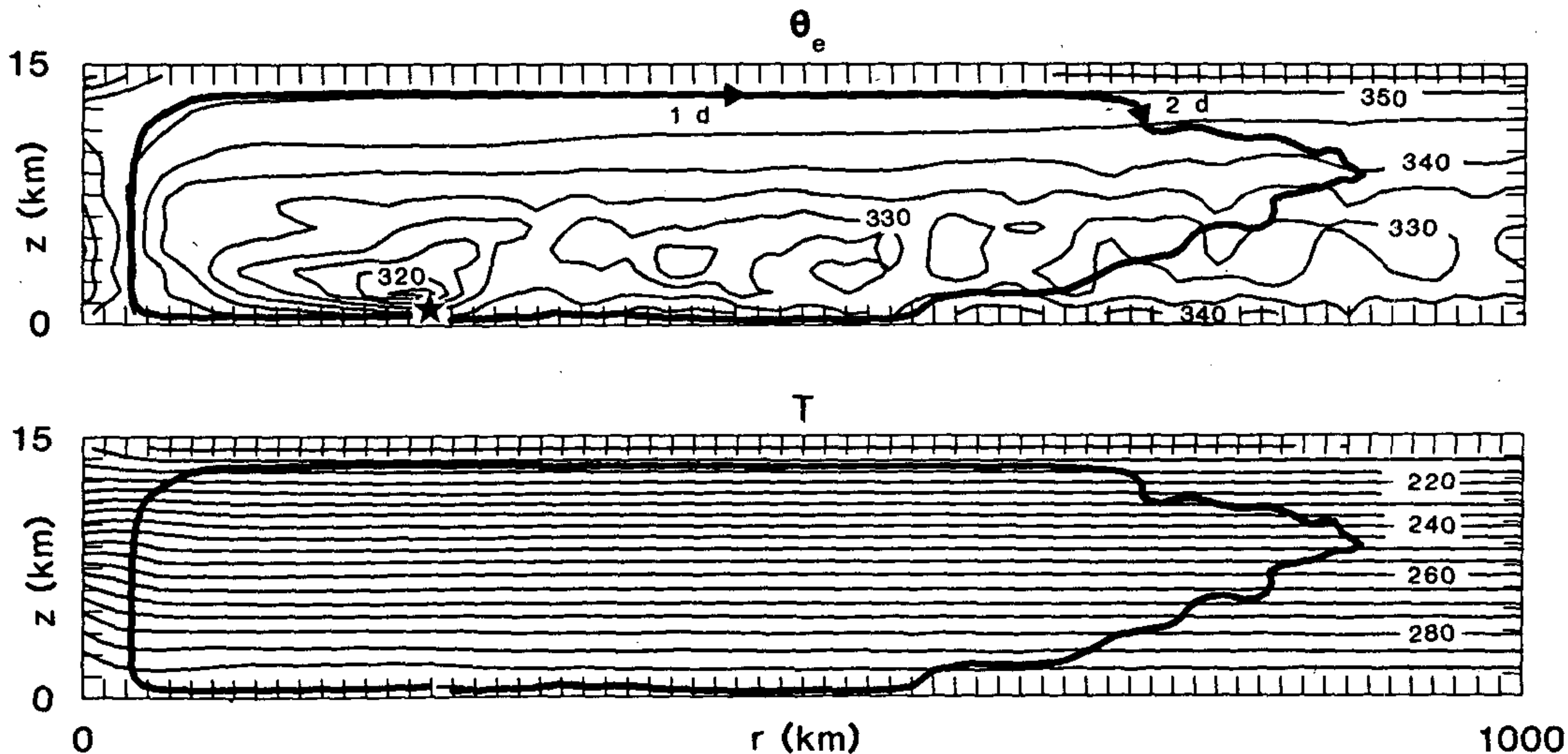
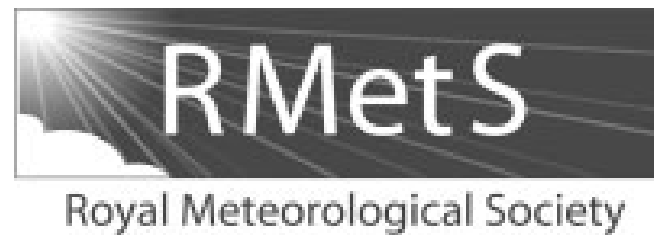


FIG. 17. An air-parcel trajectory through the eyewall, outflow layer, descent at large radius and return, superimposed on  $\theta_e$  and  $T$  in the 160–180 h averaged control run. The starting point (star) is chosen where  $\theta_e$  begins its steady inward increase ( $\theta_e \approx 340$  K); heat is acquired at constant temperature along the sea surface; the parcel rises moist adiabatically ( $\theta_e = \text{constant}$ ) and eventually descends and reaches its original value of  $\theta_e$ , thus losing its heat near the low-temperature tropopause. It takes approximately 40 d for the parcel to complete its journey back to the starting point over which time it acquires a small amount of extra heat which, we argue, it needs to overcome dissipation within cumulus clouds.



---

# Thermodynamic control of tropical cyclogenesis in environments of radiative-convective equilibrium with shear

Eric D. Rappin<sup>a\*</sup>, David S. Nolan<sup>a</sup> and Kerry A. Emanuel<sup>b</sup>

<sup>a</sup>*Rosenstiel School of Marine and Atmospheric Science, University of Miami, Florida, USA*

<sup>b</sup>*Program in Atmospheres, Oceans and Climate, Massachusetts Institute of Technology, Cambridge, USA*

\*Correspondence to: E. D. Rappin, RSMAS/MPO, 4600 Rickenbacker Causeway, Miami, FL 33149, USA. E-mail: [erappin@rsmas.miami.edu](mailto:erappin@rsmas.miami.edu)

---

# Methodology

- Weather Research and Forecast (WRF)
- Grid spacing 3 km.
- 6-class microphysics.
- Interactive radiation.

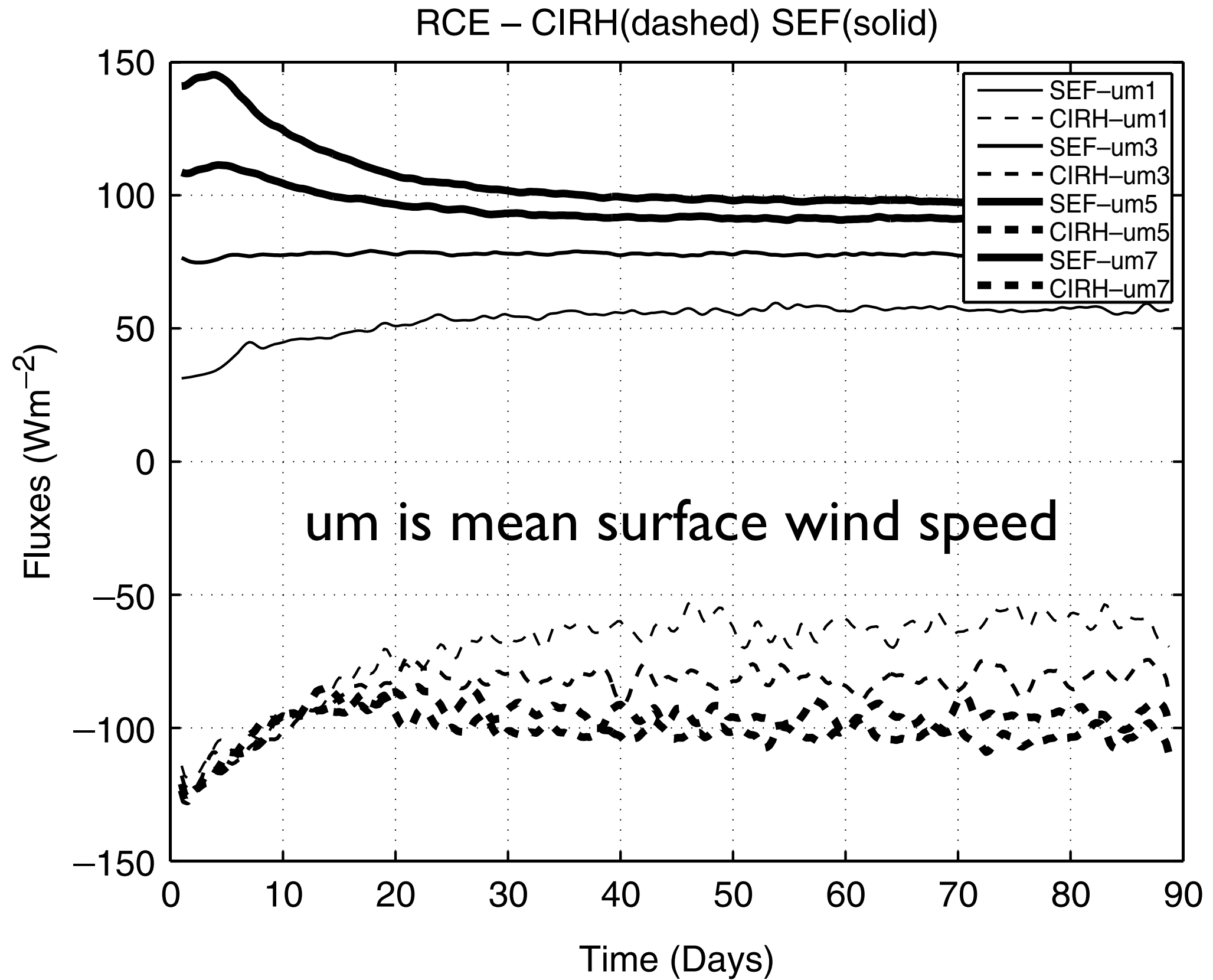


**Figure 1.** Horizontal mean of column-integrated radiative heating (CIRH, dashed) and surface enthalpy fluxes (SEF, solid). All units are  $\text{W m}^{-2}$ .

# Methodology

- Run to RCE on small domain (150 km x 150 km).
- Use RCE state with a 10 m/s, mid-level, cold-core vortex on a 1200 km x 1200 km doubly cyclic domain.
- Simulate tropical cyclogenesis.

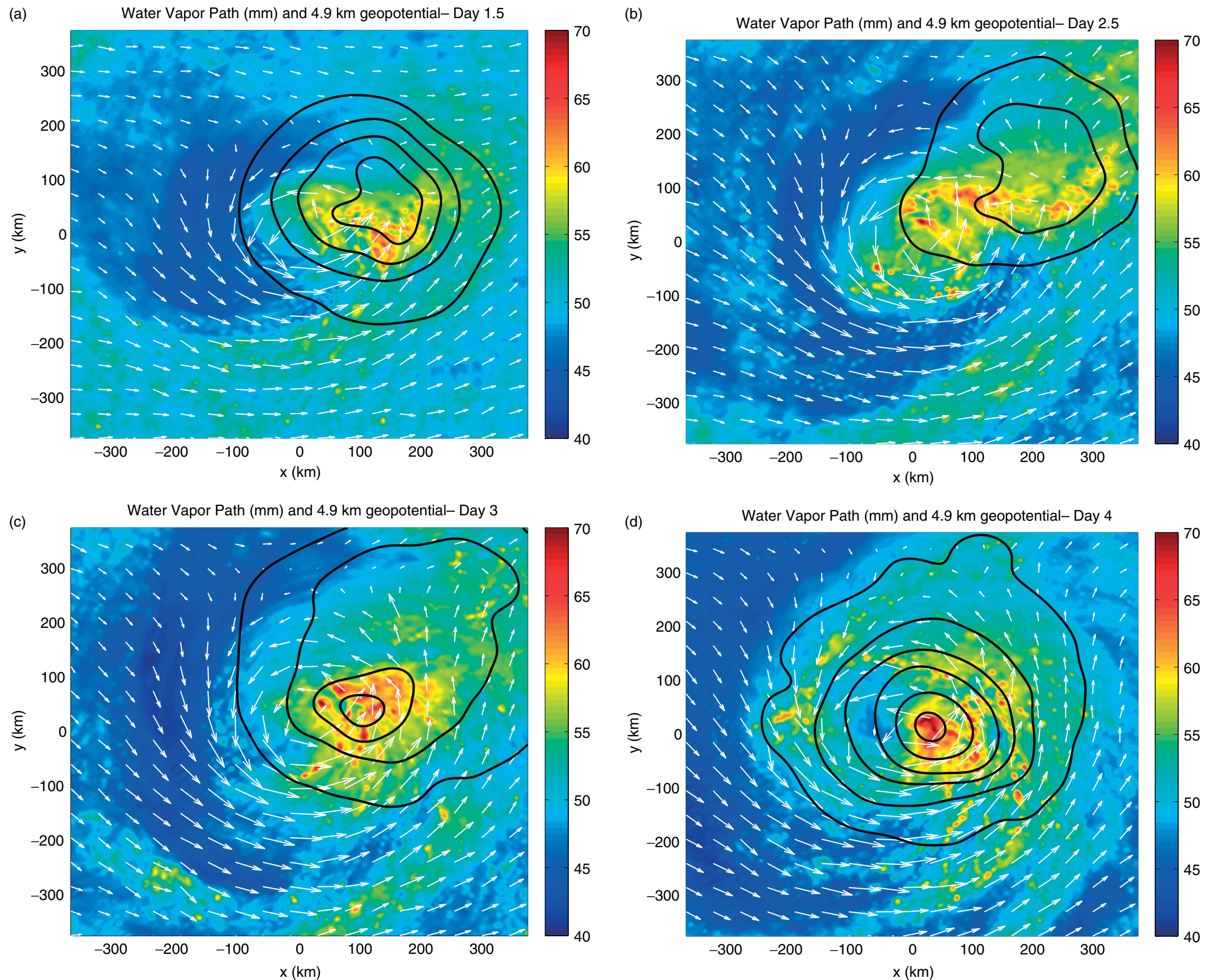


**Figure 8.** Experiment CONTROL: water vapour path (mm, shading), surface wind (vectors), and  $\phi$  at 550 hPa (contours decreasing inwards: 4.875, 4.870, 4.865, 4.860, 4.850, 4.835 km) for (a) 1.5 days, (b) 2.5 days, (c) 3 days, and (d) 4 days. The  $700 \text{ km} \times 700 \text{ km}$  region shown is less than that of the entire model domain, and is centred on the surface vortex.

